

# Milky Way mass galaxies with X-shaped bulges are not rare in the local Universe

Laurikainen E.<sup>1, 2\*</sup>, Salo H.<sup>1</sup>, Athanassoula E.<sup>3</sup>, Bosma A.<sup>3</sup>, Herrera-Endoqui M.<sup>1</sup>

<sup>1</sup>*Dept of Physics/Astronomy Division, University of Oulu, FIN-90014, Finland*

<sup>2</sup>*Finnish Centre of Astronomy with ESO (FINCA), University of Turku, Väisäläntie 20, FI-21500 Piikkiö, Finland*

<sup>3</sup>*Aix Marseille Université, CNRS, LAM (Laboratoire d’Astrophysique de Marseille) UMR 7326, 13388, Marseille, France*

Accepted: Received:

## ABSTRACT

Boxy/Peanut/X-shaped (B/P/X) bulges are studied using the 3.6  $\mu\text{m}$  images from the Spitzer Survey of Stellar Structure in Galaxies (S<sup>4</sup>G), and the K<sub>s</sub>-band images from the Near-IR S0 galaxy Survey (NIRS0S). They are compared with the properties of barlenses, defined as lens-like structures embedded in bars, with sizes of  $\sim 50\%$  of bars and axial ratios of  $\sim 0.6$ - $0.9$ . Based on observations (extending Laurikainen et al.) and recent simulation models (Athanassoula et al.) we show evidence that barlenses are the more face-on counterparts of B/P/X-shaped bulges. Using unsharp masks 18 new X-shaped structures are identified, covering a large range of galaxy inclinations. The similar masses and red B-3.6 $\mu\text{m}$  colors of the host galaxies, and the fact that the combined axial ratio distribution of the host galaxy disks is flat, support the interpretation that barlenses and X-shapes are physically the same phenomenon. In Hubble types  $-3 \leq T \leq 2$  even half of the bars contain either a barlens or an X-shaped structure. Our detailed 2D multi-component decompositions for 29 galaxies, fitting the barlens/X-shape with a separate component, indicate very small or non-existent classical bulges. Taking into account that the structures we study have similar host galaxy masses as the Milky Way (MW), our results imply that MW mass galaxies with no significant classical bulges are common in the nearby Universe.

## Key words:

galaxies: structure - galaxies: evolution - galaxies: bulges - galaxies: spiral galaxies: elliptical and lenticular, cD

## 1 INTRODUCTION

Understanding the formation of bulges is a key in any model of galaxy formation and evolution. The main types of bulges are classical bulges formed in the primordial galaxies or by galaxy mergers, and bulges formed by secular processes (Kormendy & Kennicutt 2004). One type of non-classical bulges forms via bar induced gas inflow, followed by star formation, which can be interpreted as small inner disks (“disky bulges” by Athanassoula 2005). Or they can be Boxy/Peanut (B/P) bulges (Combes & Sanders 1981; Athanassoula & Misiornis 2002), being actually vertically thick inner parts of bars seen edge-on (Lütticke, Dettmar & Pohlen 2000). In unsharp mask images they often show X-shapes (Bureau et al. 2006), and are collectively called as B/P/X-shaped structures.

The “disky bulges” have apparent flattening similar to that of the disk (Kent 1985), blue optical colors, and Sérsic

indexes indicative of nearly exponential surface brightness profiles (Drory & Fisher 2007). B/P/X bulges form part of the bar and therefore are expected to have similar colors as the inner disk. Classical bulges have old stellar populations and enhanced  $[\alpha/\text{Fe}]$  abundances (MacArthur, González & Courteau 2009; Sánchez-Blázquez et al. 2011). However, it is not easy to distinguish classical and secularly formed bulges based on their colors or ages. Bulges can be re-juvenated by inflow of gas via cosmic filaments, wet minor mergers, or cooling gas from the baryonic halos, giving a mixture of stellar ages and abundances (Coelho & Gadotti 2011; Pérez, Sánchez-Blázquez & Zurita 2009), and complex stellar kinematics (Mendez-Abreu et al. 2008; Williams et al. 2011). The mechanisms that re-juvenate bulges can also make them flatter and faster rotating (Khochfar et al. 2011). Classical bulges, covering a large range of bulge-to-total ( $B/T$ ) flux ratios, can be qualitatively reproduced by the current cosmological simulations within the hierarchical galaxy assembly (Kauffman 1996; Governato et al. 2007).

\* E-mail: eija.laurikainen@oulu.fi

Nevertheless, more quantitative analysis has shown that in cosmological simulations the cumulative effects of adding mass to the bulge and increasing its Sérsic index during the galaxy evolution are easily overestimated (Silk, Di Cintio & Dvorkin 2013 and references therein). Many high redshift galaxies, in the environment where bulge formation is expected to be vigorous, show clumpy morphologies without any clear central mass concentrations (Förster Schreiber et al. 2009, 2011). Also, analysis of the  $B/T$  flux-ratios in the local Universe (Laurikainen et al. 2005, 2010, Graham & Worley 2008, Gadotti 2009, Kormendy et al. 2010, Weinzirl et al. 2009) show systematically less massive bulges than predicted by cosmological simulations.

In this study we take a new approach to analyze bulges/inner bar components, deriving even stricter limit for the fraction of light in classical bulges. The central ingredient is to correctly account for the *barlens* (bl) component, as its light is often erroneously attributed to a classical bulge. Barlenses, e.g. lens-like structures embedded in bars were identified as distinct structural features by Laurikainen et al. (2007, 2011), where it was also speculated that they are vertically extended features forming the inner parts of bars. This conjecture is shown to be true for the barlens component of simulated galaxies in Athanassoula et al. (2014). In this letter we give further evidence showing that observed barlenses, appearing in fairly face-on galaxies, are physically the same phenomenon as the B/P/X-shaped bulges in more inclined galaxies.

## 2 SAMPLE AND DATA ANALYSIS

### 2.1 Sample

We use 3.6  $\mu\text{m}$  images of the Spitzer Survey of Stellar Structure in Galaxies ( $S^4\text{G}$ , Sheth et al. 2010), which is a sample of 2352 nearby galaxies, covering all Hubble types and disk inclinations with total blue magnitude  $B_T \leq 15.5$  mag. Our other database is the Near-IR S0-Sa galaxy Survey (NIRS0S, Laurikainen et al. 2011) of 206 early-type disk galaxies observed at  $K_s$ -band, with  $i \leq 65^\circ$ . Because  $S^4\text{G}$  contains only galaxies with HI emission, a sample combined with NIRS0S guarantees that also early-type disk galaxies lacking gas are included: NIRS0S contains 113 galaxies not in  $S^4\text{G}$ , leading to the total number of 2465 galaxies. As we are interested in the relative masses of the structural components, near and mid-IR images are used, tracing the old stellar populations (see Meidt et al. 2012).

Our combined sample contains 80 barlenses and 89 X-shaped (or B/P) structures, based on the morphological classifications by Laurikainen et al. (2011) and Buta et al. (2014), or found in our unsharp mask analysis described below. These numbers not necessarily contain all bulges with boxy isophotes. In our statistical analysis we limit to  $B_T \leq 12.5$  mag, which is the NIRS0S completeness limit: this leaves  $N = 597$  galaxies (99 from NIRS0S): 365 are barred (SB or SAB), 42 host X-shapes and 61 have barlenses, indicating an overall X/bl fraction of 28% among barred galaxies. As NIRS0S galaxies have  $i \leq 65^\circ$  we probably lack some gas poor high inclination systems with B/P/X-shapes. Based on the frequency of B/P/X-shapes among highly inclined early-type  $S^4\text{G}$  galaxies, we estimate that at most  $\sim 10$  such galaxies are missing from our mag-limited subsample.

### 2.2 Unsharp masking and multi-component decompositions

In order to be sure that all X-shapes are found, unsharp masks were created for all  $S^4\text{G}$  and NIRS0S galaxies. We convolved the images with a Gaussian kernel (width 5-20 pix), and divided the original image with the convolved image. As a result 18 new X-shapes were discovered.<sup>1</sup>

We perform detailed multi-component decompositions on 30 galaxies (with  $i \leq 65^\circ$ ), of which 15 have barlenses and 14 X-shaped structures. Separate components are included for the inner (bl/B/P/X) and the outer thin bar components, and the main emphasis is to see how this affects the derived bulge component. The decompositions were carried out using GALFIT (Peng et al. 2010), with the help of IDL-based GALFIDL-procedures (Salo et al. 2014). We use a Sérsic function for the bulge, disk, and the inner bar components, and Ferrers function for the outer bar. If needed, an extra unresolved central source is also added. In distinction to the starting models, taken from Laurikainen et al. (2010) for NIRS0S, and from Salo et al. (2014) for  $S^4\text{G}$ , the shape parameters  $\alpha$  and  $\beta$  in the Ferrers function, and the boxy/disciness of the isophotes were all left free in the fit. The use of a Sérsic function for the disk guaranteed that also Freeman type II profiles with disk breaks or non-exponential surface brightness profiles are fitted in a reasonable manner.

## 3 RESULTS AND DISCUSSION

### 3.1 Barlenses - face-on counterparts of B/P/X-shaped “bulges”

B/P/X-shaped bulges (Combes & Sanders 1981; Pfenniger & Friedli 1991; Athanassoula 2005) have been extensively discussed in galaxies seen edge-on. Simulation models have also shown that B/P-bulges can develop X-shapes when the bar grows in strength (see Athanassoula 2005). Athanassoula & Beaton (2006) showed that such bulges are visible not only in the edge-on geometry, but also in fairly inclined galaxies, using isophotal analysis. This was extended Erwin & Debattista (2013) to moderately inclined galaxies, applied to a sample of 78 galaxies.

Barlenses (though not yet called as such) were speculated to be the nearly face-on counterparts of B/P/X-shaped structures by Laurikainen et al. (2007). In distinction to classical bulges barlenses have flatter light distributions, and in distinction to nuclear lenses they are larger, covering  $\sim 50\%$  of the bar size (Laurikainen et al. 2011, 2013). No theoretical proof for this existed at that time. In Athanassoula et al. (2014) we identify barlens components in N-body + SPH simulations, and find a good agreement with observed barlenses. Moreover, by comparing views from different directions, this study shows that the simulated barlenses and B/P/X bulges are indeed the same component.

<sup>1</sup> The new X-shape detections are: ESO404-027, ESO443-042, IC0335, IC1067, IC3806, NGC0522, NGC0660, NGC1476, NGC3098, NGC4856, NGC5022, NGC5145, NGC5375, NGC5806, NGC7513, NGC3692, NGC5145, NGC5757. Some of these galaxies were identified as B/P in Buta et al. (2014).

An example of the good correspondence between simulations/observations is illustrated in Figure 1, which compares the NIRS0S image of NGC 4314 (a prototypical barlens galaxy) with a simulation model from Athanassoula et al. (2013). Along the bar major axis the barlens connects smoothly into the thin bar. There is also a central peak which in principle could be a separate small bulge. However, at least in this case it is clear that the bulge is by no means a classical bulge, as the 'bulge' region contains several disk-specific structures (see Benedict et al. 1993, 2002; Erwin & Sparke 2003). A comparison with the simulation model also shows a remarkable similarity of the profiles, including the central peak which in the model forms part of the bar (the model does not include any separate bulge component).

As a further evidence supporting this conjecture, we find that the combined axial ratio distribution of the galaxies with barlenses and X-shaped structures is flat (Fig. 2a), suggesting that these structures indeed are physically the same phenomenon. Consistent with this idea is that both types of bars reside in massive galaxies (Fig. 2b) with similar red  $B$ -3.6  $\mu\text{m}$  (AB) colors. The median masses of the host galaxies are  $\log M^*/M_\odot = 10.57$  and 10.52, and the colors 1.25 and 1.26, for the barlens and X-shaped galaxies, respectively. Barlenses appear shifted towards earlier Hubble types (see Fig. 2c; MW has  $T=3$ ), but most likely this is simply a matter of classification bias: barlenses are easily confused with classical bulges and thus the hosts are assigned an earlier type. This is in accordance with the simulation models (Athanassoula et al. 2014, see Fig. 1 lower left panel) which suggest that a given model may appear to possess an extended round central component in near face-on view, which however is much less pronounced when viewed edge-on. Interestingly, the masses in Figure 2b are comparable to that of the MW, with  $\log M^*/M_\odot = 10.7$  (Flynn et al. 2006). The X-shaped inner bar component in MW (Nataf et al. 2010; Ness et al. 2012; Wegg & Gerhard 2013) is also very similar to the X-shaped structures of our sample galaxies. It has been suggested that MW has no classical bulge.

In our classification the inner component of the bar is either a barlens or an X-shape. In particular in the overlapping region in Figure 2a, the assigned class might depend on the strength of the X-shape. Figure 3 shows examples of galaxies with/without prominent X-structures, both at high and intermediate inclinations. The upper row shows two strongly X-shaped bars with  $i \approx 90^\circ$  (NGC 3628) and with  $i=45^\circ$  (IC 5240). In both cases the X-shape is clear even in the original image. The lower row shows a boxy bulge with only a weak X-shape detected in unsharp mask (NGC 4565,  $i \approx 90^\circ$ ) and a barlens (NGC 4643,  $i=37^\circ$ ). The barlens has the same appearance as the boxy bulge (with a weak X-shape) might have at the same inclination. Clearly, the classification as barlens or X-shape depends on both inclination and the prominence of the structure.

It is of interest to compare our morphological B/P/X/bl frequency to earlier studies made using either low or high-inclination samples. Erwin & Debattista (2013) made isophotal analysis for moderately inclined galaxies ( $i < 65^\circ$ ) in the Hubble type range  $-3 \leq T \leq 2$  and found that 31% of barred galaxies show boxy or spurs morphology. Using the same type/inclination range our magnitude-limited subsample has an even higher frequency: 46% of barred galaxies ( $N_{bar}=134$  out of  $N_{tot}=223$ ) have either barlenses or

X-shapes ( $N_{bl}=53$ ,  $N_X=9$ ). Relaxing the inclination limit gives, as it should, practically similar high frequency (51%;  $N_X=35$ ,  $N_{bl}=55$ ,  $N_{bar}=175$ ). Our X/bl frequency is similar to the overall fraction of 45% of B/P bulges found by Lütticke et al. (2000) among the edge-on galaxies of all Hubble types. However, in contrast to Lütticke et al. (2000), our fraction drops to zero beyond  $T = 5$  (10% for  $T=3-5$ ), whereas in their study the fraction stays over 40% even for  $T = 7$ , probably due to weak B/Ps becoming dominant.

### 3.2 Decomposing the relative fluxes of bulge/bl/B/P/X-shaped structures

If bars (thin bar + bl/X-structure) can account for most of the inner surface brightness, we may well ask how much room is left for massive classical bulges in these systems? We tackle this question by detailed structural decompositions.

Examples of our decompositions for barlens (NGC 4643) and X-shaped (IC 5240) galaxies are shown in Fig. 4. For NGC 4643 a separate bulge is fitted ( $n=0.7$ ), resulting to  $B/T \sim 0.1$ . In IC 5240 the few central pixels, fitted with the PSF, contain only  $\sim 1\%$  of the flux, indicating that this galaxy has no separate bulge. Collecting all decompositions we find  $\langle B/T \rangle \sim 0.1$  and  $n \sim 1.5$  for both types. As a large majority of the decomposed galaxies are classified as early-type disks this is a very small number, corresponding to that typical for Sbc-Sc spirals (Laurikainen et al. 2010). For comparison, if the bl/X-shaped component were omitted from an otherwise similar decomposition, this results in  $\langle B/T \rangle = 0.35$ , similar to  $B/T$ 's previously obtained by Gadotti (2009) and Laurikainen et al. (2007, 2010)<sup>2</sup>, though Laurikainen et al. (2007, 2010) made also more complex decompositions resulting to lower  $B/T$ -values.

In the current decompositions barlenses and X-shaped components account for relative fluxes of  $\langle F(\text{bl})/F(\text{tot}) \rangle = 0.18 \pm 0.11$  and  $\langle F(X)/F(\text{tot}) \rangle = 0.08 \pm 0.02$ . The fact that barlenses appear marginally more prominent could be a selection effect: even weak X-shapes stand out in edge-on galaxies, whereas a small barlens is hard to identify reliably and is thus more easily discarded from classification.

In Figure 5 we further show that both  $F(\text{bl})/F(\text{thin bar})$  and  $F(\text{bl})/F(\text{tot})$  correlate with bar strength ( $A_2$ ). Also, barlenses seem to be fairly round, e.g. they have large axial ratios. Clearly, a prominent barlens means also a strong bar. These correlations, as well as the rather round appearance of barlenses, are predicted by those simulation models in Athanassoula et al. (2013, 2014), which start from initial conditions including gas.

## 4 SUMMARY AND IMPLICATIONS

We have shown observational evidence that barlenses are the more face-on counterparts of the vertically thick B/P/X-shaped bar structures, in a good agreement with the simulations by Athanassoula et al. (2014). Consistent with this idea is that the host galaxy properties of both structures

<sup>2</sup> It has been shown previously that completely omitting the bar in the fit would further increase the relative mass erroneously assigned to the bulge (Laurikainen et al. 2006).

are similar, having similar masses and red B-3.6 $\mu$ m colors. Also, together the two types of galaxies form a flat axial ratio distribution. Barlenses appear shifted towards earlier Hubble types, most likely because in galaxy classifications they are mistaken with classical bulges. Accounting for their central components as bulges leads to  $\langle B/T \rangle \sim 0.1$  and  $\langle n \rangle \sim 1.5$  in both types, inconsistent with the classical bulge picture. According to our analysis,  $\sim 50\%$  of early type ( $-3 \leq T \leq 2$ ) bars contain a B/P/X/bl structure.

Our results are consistent with many observations of bulges, which are often interpreted to cover the same galaxy regions as the vertically thick inner bar components. Almost all bulges are fast rotating (Cappellari et al. 2011, 2013). Many explanations exist for that, but the observation fits also to our interpretation where the vertically thick inner bar regions form part of the bar, rotating in a similar manner as the rest of the disk. The observation that bulges in the early-type disk galaxies are generally red (Driver et al. 2006) also naturally fits into our interpretation, because bars often have old stellar populations (Pérez, Sánchez-Blázquez & Zurita 2009). The major implications are:

1. *Milky Way mass galaxies having no classical bulges are common in the nearby Universe.* This result seems to hold even for early-type disk galaxies where the most massive classical bulges are assumed to reside.

2. *Our results put strong constraints to those galaxy formation models in which massive classical bulges form in the early Universe.* Either the massive classical bulges formed at high redshifts have been destroyed at some stage of galaxy evolution, or in many barred galaxies they never formed.

## ACKNOWLEDGMENTS

EL and HS acknowledge financial support from the Academy of Finland, EA and AB from the CNES, and all from EU grant PITN -GA-2011-289313 (DAGAL EU-ITN network). We thank the anonymous referee of valuable comments.

## REFERENCES

Athanassoula E., Misiroidis A., 2002, MNRAS, 330, 35  
 Athanassoula E., 2005, MNRAS, 358, 1477  
 Athanassoula E., Beaton R. 2006, MNRAS, 370, 1499  
 Athanassoula E. et al. 2013, MNRAS, 429, 1949  
 Athanassoula et al., 2014, astro-ph 1405.6726  
 Benedict C.F. et al. 1993, AJ, 105, 1369  
 Benedict C.F. et al. 2002, AJ, 123, 1411  
 Buta R. et al., in preparation  
 Bureau M. et al., 2006, MNRAS, 370, 753  
 Cappellari et al., 2011, MNRAS, 416, 1680  
 Cappellari et al., 2013, MNRAS, 432, 1862  
 Coelho P., Gadotti D.A., 2011, ApJ, 743, 13  
 Combes F., Sanders R.H., 1981, AA, 96, 164  
 Driver S. et al., 2006, MNRAS, 368, 414  
 Drory N., Fisher D., 2007, ApJ, 664, 640  
 Erwin P., Sparke L. S. 2003, ApJS, 146, 299  
 Erwin P., Debattista V., 2013, MNRAS, 431, 3060  
 Flynn C. et al., 2006, MNRAS, 372, 1149  
 Förster Schreiber et al., 2009, ApJ, 706, 1364  
 Förster, Schreiber et al., 2011, ApJ, 739, 45

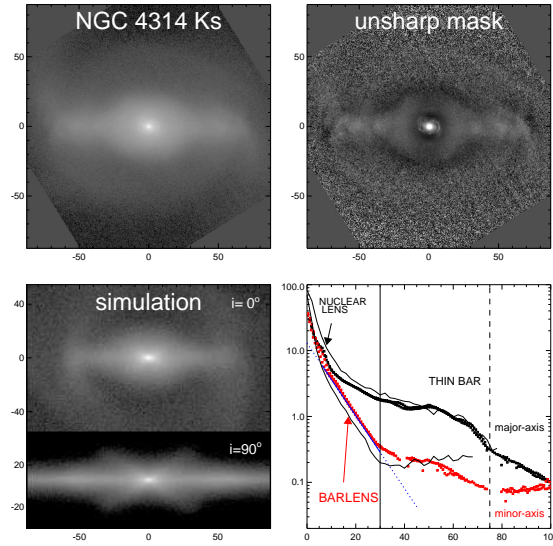


**Figure 1.** An example of a barlens galaxy NGC 4314, showing the original K<sub>s</sub>-band image (from Laurikainen et al. 2011), the unsharp mask image, and the surface brightness profile along the bar major and minor axis (symbols). The lower left panel shows the simulation model gtr115 from Athanassoula et al. (2013), both in face-on and edge-on view. The simulation model profiles are also shown by solid lines in the profile plot. Axis labels are in arcseconds in all panels.

Gadotti, D. 2009, MNRAS, 393, 1531  
 Governato F. et al. 2007, MNRAS, 374, 1479  
 Graham A., Worley C.C., 2008, MNRAS, 388, 1708  
 Kauffman G. 1996, MNRAS, 281, 487  
 Kent S.M., 1985, ApJS, 59, 115  
 Khochfar et al., 2011, MNRAS, 417, 845  
 Kormendy J. et al., 2010, ApJ, 723, 54  
 Kormendy J., Kennicutt R., 2004, ARA&A, 42, 603  
 Laurikainen E. et al., 2005, MNRAS, 362, 1319  
 Laurikainen E. et al., 2006, AJ, 132, 2634  
 Laurikainen E. et al., 2007, MNRAS, 381, 401  
 Laurikainen E. et al., 2010, MNRAS, 405, 1089  
 Laurikainen E. et al., 2011, MNRAS, 418, 1452  
 Laurikainen E. et al., 2013, MNRAS, 430, 3489  
 Lütticke R., Dettmar R., Pohlen M., 2000, AAS, 145, 405  
 MacArthur L. et al. 2009, MNRAS, 395, 28  
 Méndez-Abreu J. et al., 2008, ApJ, 679, L73  
 Meidt et al., 2012, ApJ, 744, 17  
 Nataf et al. 2010, ApJ, 721L, 28N  
 Ness et al. 2012, ApJ, 756, 22  
 Peng C., Ho L., Impey C., Rix H-W, 2010, AJ, 139, 2097  
 Pfnegger D., Friedli D., 1991, AA, 252, 75  
 Pérez I. et al. 2009, AA, 495, 775  
 Salo, H. et al., in preparation  
 Sheth et al. 2010, PASP, 122, 1397  
 Silk J., Di Cintio A., Dvorkin I., 2013, astro-ph 1312.0107  
 Sánchez-Blázquez P. et al., 2011, MNRAS, 415, 709  
 Wegg C., Gerhard O., 2013, MNRAS, 435, 1874  
 Weinzirl T. et al., 2009, ApJ, 696, 411  
 Williams M. et al., 2011, MNRAS, 414, 2163

This paper has been typeset from a T<sub>E</sub>X/L<sup>A</sup>T<sub>E</sub>X file prepared by the author.

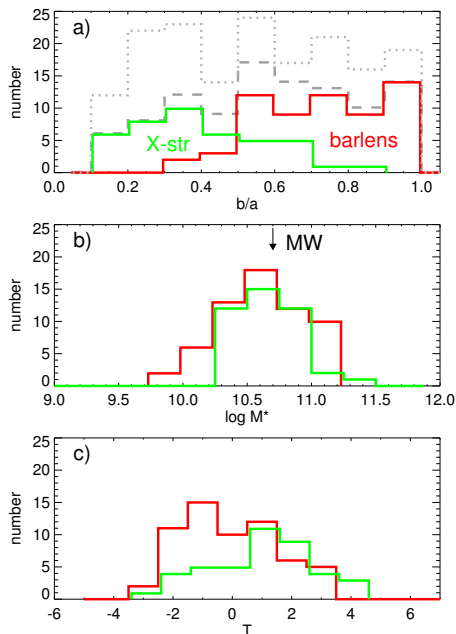


**Figure 2.** The distributions of (a) galaxy minor-to-major ( $b/a$ ) axis ratios, (b) total stellar masses (in units of solar masses) and (c) Hubble types  $T$  of the galaxies hosting either barlenses (red) or X-shaped structures (green). In these plots the magnitude-limited ( $B_T \leq 12.5$  mag) subsample is used ( $N_{tot} = 597, N_{bar} = 365, N_X = 42, N_{bl} = 61$ ). In a) also the combined barlenses+X-shape distribution is shown, both for the above sample (dashed line) and for the original sample of  $N=2465$  galaxies. The dotted line shows all bl+X-shapes of the full combined sample. The stellar masses are calculated as in Munoz-Mateos et al. (2013) for S<sup>4</sup>G. Note that the potentially missing gas-poor, early type,  $i > 65^\circ$  galaxies with X-shapes would further flatten the  $b/a$  distribution.

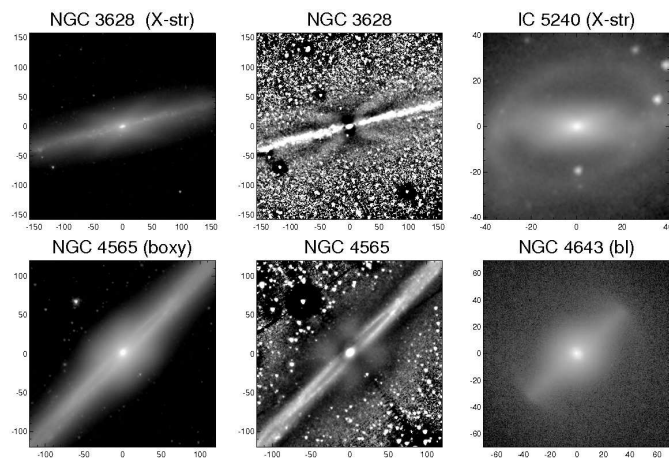


**Figure 3.** Upper row shows two X-shaped galaxies, NGC 3628 and IC 5240, and the lower row boxy/barlens galaxies, NGC 4565 and NGC 4643. In the left panels the galaxies are nearly edge-on, whereas in the right panels the inclinations are  $45^\circ$  and  $37^\circ$  for IC 5240 and NGC 4643, respectively. The middle panels show the unsharp mask images of the edge-on galaxies. The unsharp masks for IC 5240 and NGC 4643 are shown in Figure 4. The images of NGC 4643 and IC 5240 are from NIRS0S, the other two galaxies are from S<sup>4</sup>G.

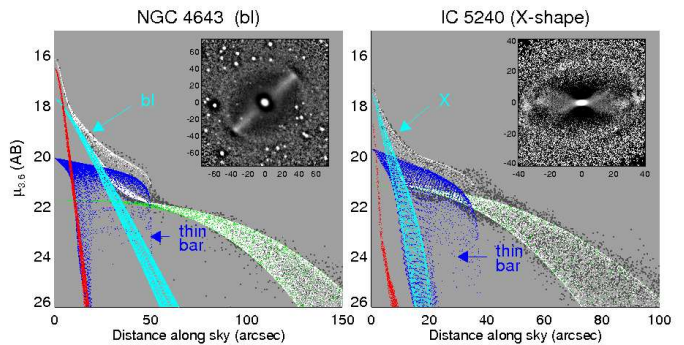


**Figure 4.** Decomposition models for the barlenses and X-shaped galaxies NGC 4643 and IC 5240, for which galaxies the images are shown in Figure 3. Black dots are the pixel values of the two-dimensional images, and white dots show the pixel values of the decomposition models. Red and green dots show the bulge and the disk components, whereas the dark and light blue indicate the thin and thick bar (bl or X) components. See the details of the models in the text. The inserts show the unsharp mask images. These decompositions use  $3.6\mu\text{m}$  images, but the bulge parameters are similar when using  $K_s$ -band images. The mean Hubble types for the decomposed bl and X-shaped galaxies are  $\langle T \rangle = -0.75$  and  $1.2$ , respectively.

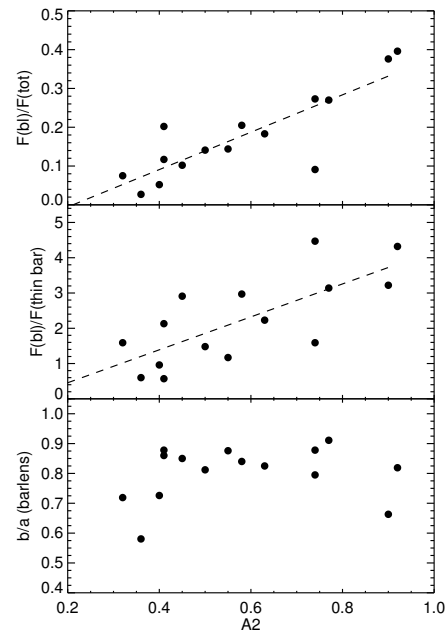


**Figure 5.** Observed relative fluxes of barlenses are shown as a function of  $A_2$ , for all those barlenses galaxies for which decompositions were made in this study.  $A_2$  is the peak value of the  $m=2$  Fourier amplitude of density in the bar region. In the upper panel the flux is normalized to the total galaxy flux ( $F(\text{bl})/F(\text{tot})$ ), and in the middle panel to the flux of the thin bar component ( $F(\text{bl})/F(\text{thin bar})$ ). Lower panel shows the observed axial ratio of the barlenses,  $b/a$ , as a function of  $A_2$  for the same galaxies. The axial ratios are from Laurikainen et al. (2011).